Transportation Research Part D 130 (2024) 104178

Contents lists available at ScienceDirect

Transportation Research Part D

journal homepage: www.elsevier.com/locate/trd

Allocate electric vehicles' public charging stations with charging demand uncertainty

Ting Wu [a], Emily Fainman [b,*], Yasmina Maïzi [c], Jia Shu [d], Yongzhen Li [e]

[a] Department of Mathematics, Nanjing University, 22 Hankou Road, Nanjing, 210093, Jiangsu, China
[b] McCoy College of Business, Texas State University, 601 University Drive, San Marcos, 78666, TX, USA
[c] École des Sciences de la Gestion, Université du Québec à Montréal, 315 St Catherine St E, Montreal, H2X 3X2, Quebec, Canada
[d] School of Management and Economics, University of Electronic Science and Technology of China, 2006 Xiyuan Avenue, Chengdu, 611731, Sichuan, China
[e] Department of Management Science and Engineering, School of Economics and Management, Southeast University, 2 Sipai Road, Nanjing, 210096, Jiangsu, China

ARTICLE INFO

Keywords:
Robust optimization
Allocation problem
Electric vehicle charging infrastructure
Discrete-event simulation

ABSTRACT

Nowadays, electric vehicles (EVs) have developed rapidly due to their great advantages in fuel savings, reduced greenhouse gas emissions, and low air pollution. However, charging imbalances and shortages have limited the prevalence of EVs. We optimize the siting and sizing of public charging stations under uncertain urban en-route recharging demand. Considering charging congestion, we introduce the Erlang's loss formula to represent the service level requirement of each charging station. First, we determine the optimal locations and sizes of those stations by a robust optimization model, where we figure out its deterministic dual following linear approximation of the loss rate in queueing models. We further use a discrete-event simulation to relax the assumption of time-independent charging demand in the optimization approach and model real-time traffic based on real-world traffic and power grid information in Nanjing, China. Thus, we verify the robust optimum outperforming deterministic and stochastic optimums.

1. Introduction

The global transition to electric vehicles (EVs) represents a pivotal shift toward sustainable transportation, promising reduced emissions and decreased dependence on fossil fuels. However, despite significant advancements in battery technology and the proliferation of financial incentives, EV adoption remains in its nascent stages, characterized by a limited number of users worldwide. Amidst discussions surrounding factors influencing EV prevalence, such as government subsidies and technological innovations, the significance of public charging infrastructure often remains underestimated. For instance, recent studies by Hall and Lutsey (2017) and Islam et al. (2018) shed light on the pivotal role of public charging infrastructure in shaping EV awareness and instilling confidence in potential users. Currently, two primary en-route charging options exist: battery swap stations (BSS) – allowing users to exchange exhausted batteries with fully charged ones – and public EV charging infrastructure. While BSS confronts challenges such as battery standardization, infrastructure preparedness, and financial investment requirement (Setiawan et al., 2023), several leading EV manufacturers to abstain from adopting this option for now,[1] the need for accessible and reliable public EV charging infrastructure becomes increasingly imperative.

* Corresponding author.
E-mail address: c_z88@txstate.edu (E. Fainman).

[1] See https://www.teslarati.com/tesla-shuts-down-battery-swap-program-for-superchargers/ (retrieved on 2019-02-26).

https://doi.org/10.1016/j.trd.2024.104178
Received 9 August 2023; Received in revised form 13 February 2024; Accepted 19 March 2024
Available online 6 April 2024

To address the diverse needs of EV users, charging infrastructure is typically categorized into three tiers: level 1, level 2, and direct current fast chargers (DCFCs) (Union of Concerned Scientists, 2018). While level-1 chargers primarily cater to household use, level-2 and DCFCs are deployed in public spaces, with DCFCs offering faster charging options yet 10–15 times more expensive than level-2 chargers (Habib et al., 2017). Capable of replenishing EV batteries under 30 minutes, DCFCs are particularly sought after for en-route charging, serving long-distance drivers and individuals without overnight or workplace charging access. Drivers prioritize convenient access to DCFCs to minimize charging time during their journeys. Moreover, public DCFCs have garnered increasing national policy and financial support in major Chinese cities.[2] Therefore, we focus on optimizing the deployment of DCFCs, stations, and associated electricity grids for direct plug-in charging equipment in public spaces such as parking lots of shopping malls, railway stations, and streets.

The substantial installation costs of DCFCs pose challenges for widespread deployment, highlighting the importance of optimizing their allocation at strategic locations to maximize charging infrastructure utility. Utilization rates of current chargers vary significantly among Chinese cities, with some areas reaching up to 70%, while others exhibit extremely low rates in the same region.[3] This underscores the need for appropriate allocation. A critical challenge in optimizing DCFC deployment is accurately estimating charging demand within specific regions. Without clear projections of future EV driver populations or comprehensive insights into charging patterns and user behavior, determining the appropriate number and locations of DCFCs is daunting. To address this gap, we propose a model for a robust network of public EV charging stations with DCFCs. Our model considers uncertain charging demand estimated from real-world data on traffic flow density, as well as time-varying traffic patterns influenced by weather and seasons.

Our study, despite of using data from China, can apply to any type of EV which can be externally charged, including pure EVs and plug-in hybrid vehicles. In particular, we aim to minimize the total charging associated cost by allocating optimal numbers of DCFCs at the optimal locations to fulfill a high level of charging demand. The associated cost under consideration includes upfront investment of power transmission lines and DCFCs, as well as the value of travel times to the nearest charging stations throughout the decision period. Because travelers' charging demands are random and can vary across time, we first capture the uncertain charging demands with a robust optimization model. To account for potential waiting times at fully occupied charging stations, we model the utilization rate of a charging station – the percentage of times chargers are utilized – using a $M/G/m/m$ queueing model, where each charging station has a specific number of chargers, and charging times follow a general distribution. However, as the resulting utilization rate follows the *Erlang-B formula* or *Erlang's loss formula* (Shortle et al., 2018), which renders the optimization problem intractable, we establish a linear relationship between a queue's arrival rate and the number of servers. This approach enables the formulation of a linear robust optimization model. After analyzing the deterministic dual of the robust optimization problem, we are able to determine the number of chargers at certain candidate stations. Next, we verify the robust optimum in realistic traffic and power networks with a comprehensive simulation approach. In the simulation model, we relax the assumption of time-independent charging demand in the optimization approach and model real-time traffic based on real-world traffic and power grid information in Nanjing, China. We contribute to the EV charging siting and sizing literature with (1) a robust optimization framework to accommodate uncertain urban en-route recharging demand, (2) a linear approximation of Erlang-B formula, which allows to reformulate the robust optimization problem for solvers, and (3) a comprehensive simulation model of realistic time-dependent charging demand to examine the effects of our proposed public charging stations.

The remainder of this paper is structured as follows. In Section 2, we review relevant literature with this study. In Section 3, we introduce the robust model, followed by the approximated linearization of loss rate constraint and its equivalent reformulation. In Section 4, we present a case study, including the comparison with different optimization models, sensitive analysis, and the simulation based on real data. Finally, we conclude this paper by discussing limitations and future research directions in Section 5.

2. Relevant literature

Our work is closely relevant with literature focused on estimating EV charging demand and allocating EV charging facilities. Specifically, we draw connections to studies using robust optimization, queueing models, and simulation approaches to address siting and sizing of EV charging infrastructure.

It is challenging to quantify EV users' charging demand or gauge its distribution, before EVs are widely prevalent. Several studies consider influential geographic and macro economic factors in estimating charging demand in specific regions, such as Arias and Bae (2016), He et al. (2016), and Wang et al. (2019). Other studies charging demand estimation by stratifying user types (Berkelmans et al., 2018), clustering users based on time periods (Wolbertus et al., 2018), applying Markov transition matrix based on historical data (Arias et al., 2017), and leveraging informatics (Yi et al., 2022). Other researches take different approaches by gauging charging demand directly in specific settings, such as parking lots (Cai et al., 2014) and highways (Bae and Kwasinski, 2011). In this study, we directly estimate expected value and variability of en-route recharging demand based on traffic flows in the network. This is because we study the charging infrastructure and its operations in a specific transportation network, macro-level factor models and their resulting demand in one region do not apply to this work.

The problem of locating EV charging stations has been widely studied in the literature. We refer to Shen et al. (2019), Kchaou-Boujelben (2021), and Kchaou-Boujelben (2021) for extensive reviews on the planning of EV charging infrastructure. Recent works

[2] See http://www.gov.cn/zhengce/zhengceku/2020-04/23/content_5505502.htm (retrieved on 2021-03-15).

[3] See http://www.nrdc.cn/Public/uploads/2019-04-20/5cbb125a31059.pdf (retrieved on 2021-03-15).

further study the planning of charging stations under various emerging applications, such as the power-grid expansion (Quddus et al., 2021), locating charging stations for the shared EV (Brandstätter et al., 2020), or a charging system with valet charging service (Li et al., 2021). Different from many EV charging facility allocation problems deal with long-distance, inter-city trips (e.g. Kınay et al., 2021; Li et al., 2022; Yılmaz and Yagmahan, 2022), electric taxi fleets (e.g. Cilio and Babacan, 2021), and existing bus systems (e.g. Azadeh et al., 2022), this paper focuses on locating charging stations within a city region, explicitly considers uncertain charging demands, and carefully captures the charging time based on queue theory.

Unlike conventional gas stations, EV charging stations subject to congestion due to limited capacity and substantial charging times. Despite queueing models can capture the randomness in charging demand and the charging process, only a few works consider charging congestion in locating EV charging stations using queueing models. Notably, several works (e.g., Jung et al., 2014; Ghamami et al., 2016) model the queueing delay as nonlinear waiting time cost components in objective functions and apply heuristics to solve the corresponding mixed integer nonlinear model. Others (e.g., Yang et al., 2017; Xie et al., 2018; Yang, 2018) model charging congestion as service level constraints, which are then linearized approximately based on the queueing theory. Besides diffusion and other traditional approximation methods for $M/G/m/m$ queues (e.g., Hokstad, 1978; Kimura, 1983; Breuer, 2008), recent works propose reflected Brownian motion (Yao, 1985; Khazaei et al., 2011) and a new steady-state probability approximation method based on Laplace transform (Khazaei et al., 2011, 2012). Despite these methods are sufficiently accurate with huge numbers of servers and overdispersed service times (the coefficient of variation of service time is greater than 1), they are intractable for our robust optimization model. In this study, we contribute to the queueing theory with an approximately linear relationship between loss rates and numbers of servers.

The exogenous and uncertain charging demand set our work relevant with robust optimization, despite a very limited number of works study the EV charging station location problems based on robust optimization. While Hosseini and Sarder (2019) develop a *robust scenario-based* model to handle uncertain EV driving range and traffic flows, works on robust queueing theory (e.g. Bertsimas et al., 2011; Bandi et al., 2015; Whitt and You, 2018) model the uncertainty in the arrivals and services via polynomial uncertainty sets, rather than assuming specific distributions. Under uncertain charging demand, other works employ robust models to optimize the infrastructure planning of EV BSS (Mak et al., 2013), to simultaneously allocate charging stations and route EVs (Schiffer and Walther, 2018), to make location-inventory decisions with electricity prices (Sun et al., 2019), and to minimize the worst-case total travel cost and unused capacity penalty (Pourgholamali et al., 2023). We follow the framework of Bertsimas and Sim (2004) and Bertsimas and Thiele (2006) to construct and solve the deterministic dual of the original robust optimization.

Our work also relates to simulation studies of traffic flows in transportation networks. Although recent efforts develop highly computational and efficient simulation models for urban transportation systems (e.g., Basile et al., 2012; Thomin et al., 2013; Shanmukhappa et al., 2018), the application of simulations to EVs remains relatively limited. Notable studies include Mallig et al. (2016), who simulate EV charging demands in Greater Stuttgart under various market penetration scenarios, and Li et al. (2016), utilizing Beijing taxi trajectory data for a time series-based simulation model to determine charging station locations. Additionally, Marmaras et al. (2017) introduces a comprehensive simulation analyzing EV driver behaviors in transportation and power networks. Some works employ simulation-based optimization models, capturing EV driver travel patterns, charging activity, and evaluating performance measures for location decisions (e.g. Xi et al., 2013; Dong et al., 2014). In contrast to existing simulation works of EVs, our simulation approach considers time-dependent traffic flows of an urban network and the user impatience, which leads to demand loss at fully occupied charging stations. The simulation model validates optimal decisions obtained from a robust optimization model by relaxing the time-independent assumption. Interested readers can refer to our recent conference proceeding (Maïzi et al., 2019) for extensive scenarios and further discussion on simulation-based approaches.

3. Robust optimization model

In Fig. 1, we illustrate the structure and organizational framework of both the methods (Section 3) and the case study (Section 4). In this section, we formulate a robust optimization problem to determine the siting and sizing of public charging stations, so that a certain percentage of EV charging demand on local roads can be satisfied (Section 3.1). Following the proposition of an approximately linear relationship between loss rates and numbers of servers in a $M/G/m/m$ queue (Section 3.2), we can derive a deterministic equivalent reformulation of the robust optimization problem (Section 3.3). Therefore, we can solve the reformulated mixed integer linear program with commercial solvers. Finally, we formulate a stochastic model as the benchmark to the robust optimization model (Section 3.4). In addition, we present notations of our models in Table 1. Estimating parameters and sources from which their values are derived will be presented in Section 4.2

3.1. Model formulation

We estimate the siting and sizing of public EV fast-charging stations by modeling each charging station as an $M/G/m/m$ queue. We extend the time-independent charging demand at charging stations to time-dependent arrivals in our simulation model (Section 4.5). Here we focus on aggregated charging demand in a specific region; thus, we consider homogeneous EV drivers who are assumed to follow the shortest-path principal and go to their nearest charging station for charging. Heterogeneous EV drivers and their different charging choices are beyond the scope of this study.

Consider the problem of locating charging stations in a set I of potential sites and setting up chargers in each station to satisfy charging demand in a set J of demand nodes. For each site $i \in I$ and demand node $j \in J$, let $Y_i \in \{0,1\}$ be the decision of whether a charging station is located in site i, $m_i \in \mathbb{Z}_+$ be the number of chargers set up in station i, and $X_{ij} \in \{0,1\}$ be the decision of

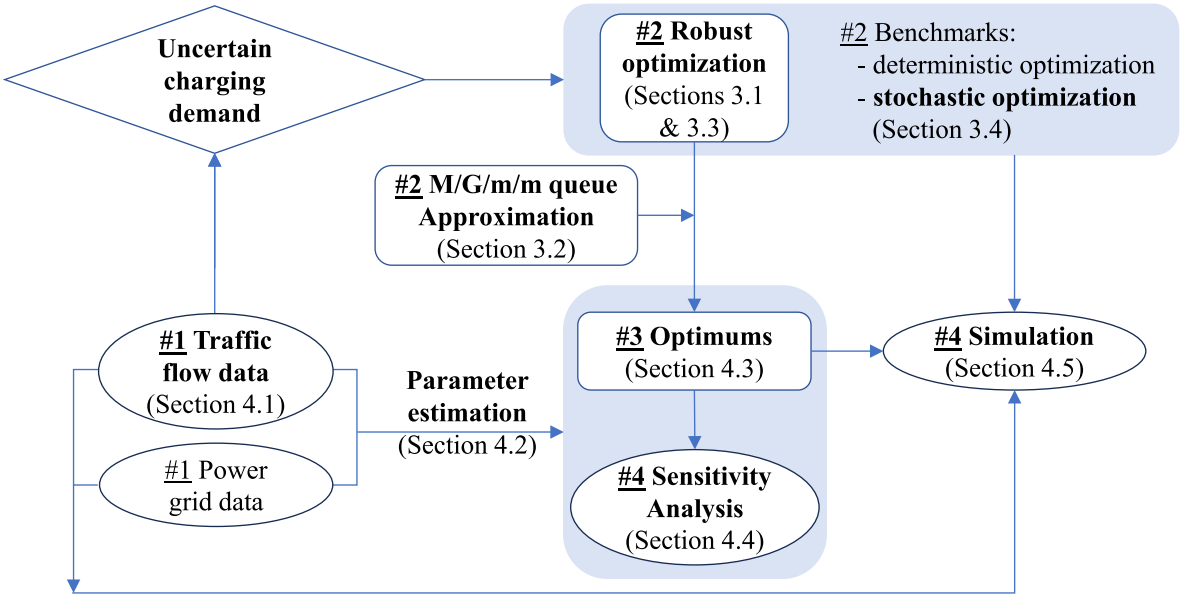

Fig. 1. The organization of the methods (Section 3) and the case study (Section 4).

whether station i serves demand node j. Denote $\boldsymbol{X}, \boldsymbol{Y}$, and $\boldsymbol{m}$ as the vectors of X_{ij}, Y_i, and m_i, respectively. The problem aims to optimize $(\boldsymbol{X}, \boldsymbol{Y}, \boldsymbol{m})$ to minimize the total cost and satisfy charging demand under certain service level requirement. For this purpose, given $(\boldsymbol{X}, \boldsymbol{Y}, \boldsymbol{m})$, the charging system in each station i is modeled by an $M/G/m_i/m_i$ queue. To be more specific, for each station i, customers (EV drivers) arrive following a Poisson process with arrival rate $\lambda_i := \sum_{j\in J} \omega_j X_{ij}$, where ω_j denotes the average charging demand rate in demand node j. Station i has m_i servers (chargers). Because EVs may have varying depleted batteries at the time of charging, we model this uncertain state-of-charge by considering servers' service (charging) time following a generally-distributed stochastic process with service rate μ. When an EV driver arrives at a station, the EV gets charged immediately if any of chargers is available, while the arriving drivers who find the system full leave immediately. In other words, waiting is not considered and the capacity of station i is m_i. In this paper, we consider the service level requirement on the loss rate of charging demand. Denote $f(\lambda_i, \mu, m_i)$ as the loss rate of the $M/G/m_i/m_i$ queue system, which is exactly the fraction of leaving customers who find the system full. According to Shortle et al. (2018), the loss rate $f(\lambda_i, \mu, m_i)$ is given by

$$f(\lambda_i, \mu, m_i) := \frac{\frac{(\lambda_i/\mu)^{m_i}}{m_i!}}{\sum_{k=0}^{m_i} \frac{(\lambda_i/\mu)^k}{k!}}. \tag{1}$$

Then, the service level requires the loss rate to be close to a preset value α, that is,

$$|f(\lambda_i, \mu, m_i) - \alpha| \le \epsilon$$

where ϵ is small but allows $m_i \in \mathbb{Z}^+$ is feasible on the set of non-negative integers.

Suppose the average demand rate ω_j is exactly known, then this charging station location problem can be modeled as

$$\min \quad \sum_{i\in I} c m_i + \sum_{i\in I} s_i Y_i + \sum_{j\in J} \omega_j \sum_{i\in I} d_{ij} X_{ij} \tag{2a}$$

$$\text{s.t.} \quad |f(\lambda_i, \mu, m_i) - \alpha| \le \epsilon, \qquad \forall i \in I, \tag{2b}$$

$$\sum_{i\in I} X_{ij} = 1, \qquad \forall j \in J, \tag{2c}$$

$$X_{ij} \le Y_i, \qquad \forall i \in I, j \in J, \tag{2d}$$

$$X_{ij}, Y_i \in \{0,1\}, m_i \in \mathbb{Z}_+, \qquad \forall i \in I, j \in J, \tag{2e}$$

The objective function (2a) minimizes the sum of three charging associated costs, namely the cost of setting up chargers $\sum_{i\in I} c m_i$, the fixed cost of setting up charging stations $\sum_{i\in I} s_i Y_i$, and the monetary value for total travel time of driving to charging stations $\sum_{j\in J} \omega_j \sum_{i\in I} d_{ij} X_{ij}$ during the time horizon of study. Constraint (2b) specifies the loss rate restriction, where the loss rate $f(\lambda_i, \mu, m_i)$ is given as in (1). Constraint (2c) requires that each demand node be served by one station. Constraint (2d) states that only the open stations can serve demand nodes.

Table 1
Model notations.

General parameters	
I	Set of potential sites to set up charging stations.
J	Set of demand nodes.
s_i	Fixed cost of setting up a charging station in site i.
c	Unit cost of setting up a charger in stations.
M_i	Maximal number of chargers that can be deployed in station i.
d_{ij}	Time cost of traveling from demand node j to station i to charge a vehicle.
ω_j	Mean charging demand rate from node j.
μ	Average service rate of a charger.
α	Service level requirement, where α represents the maximal loss rate.
β	Coefficient determined by the loss rate α.
Parameters in the queueing model (Section 3.2)	
λ_i	Arrival rate of EVs needing charging at site i.
$f(\cdot)$	Loss rate function of a $M/G/m/m$ queue.
λ	Arrival rate of a $M/G/m/m$ queue.
m	Number of servers of a $M/G/m/m$ queue.
Parameters in the robust optimization model (Section 3.3)	
$\tilde{\omega}_j$	The actual charging demand at node j.
$\bar{\omega}_j$	Nominal value of $\tilde{\omega}_j$.
$\hat{\omega}_j$	Deviation in the support of $\tilde{\omega}_j$.
$\tilde{\boldsymbol{\omega}}$	$= (\tilde{\omega}_j \ \forall j \in J)$, the vector of $\tilde{\omega}_j$.
Ω	$= \{\tilde{\boldsymbol{\omega}}\}$ the uncertainty set.
Γ	Coefficient of uncertainty level.
z_{ij}	Auxiliary variables to represent the level of uncertainty.
Z	Auxiliary variable transforming a robust optimization to a deterministic optimization.
u_j	Auxiliary variables transforming a robust optimization to a deterministic optimization.
v	Auxiliary variable transforming a robust optimization to a deterministic optimization.
p_i	Auxiliary variables transforming a robust optimization to a deterministic optimization.
q_{ij}	Auxiliary variables transforming a robust optimization to a deterministic optimization.
Parameters in the stochastic optimization (Section 3.4)	
S	Set of samples.
p^s	Probability of sample s.
$\boldsymbol{P}$	Joint distribution of $(\tilde{\omega}_j \ \forall j \in J)$.
ω_j^s	Charging demand at site j in sample s.
Decision variables	
X_{ij}	$\in \{0,1\}$. $X_{ij} = 1$ if vehicles from demand node $j \in J$ is charged in station $i \in I$ and $X_{ij} = 0$ otherwise.
Y_i	$\in \{0,1\}$. $Y_i = 1$ if a charging station is set up in potential location $i \in I$ and $Y_i = 0$ otherwise.
m_i	$\in \mathbb{Z}_+$. The number of chargers in station $i \in I$.

3.2. Linear approximation of loss rate constraint

Due to constraint (2b), model (2) is a complex nonlinear program and infeasible to solve (Tijms et al., 1981). To this end, we have the following proposition for the $M/G/m_i/m_i$ queue, which is self-contained with the subscript i dropped. Thus, we show that constraint (2b) can be approximately linearized, which leads to tractable linear approximations of model (2).

Proposition 3.1. *In the $M/G/m/m$ queue with arrival rate λ and service rate μ, if the loss rate $f(\lambda, \mu, m)$ defined in (1) is constant and m is sufficiently large, the number of servers m is approximately proportional to the arrival rate λ. In other words, if $f(\lambda, \mu, m) = \alpha$, the number of servers m is the smallest integer that is no less than $\lambda(1-\alpha)/\mu$ as $m \longrightarrow \infty$, i.e.*

$$\frac{\lambda}{m} \longrightarrow \frac{\mu}{1-\alpha}, \quad as \quad m \longrightarrow \infty. \tag{3}$$

Proof. According to Harel (1988), $f(\lambda, \mu, m)$ has the upper bound U and lower bound L such that $L \le f(\lambda, \mu, m) \le U$, $\forall \rho$, where L and U are

$$U = \frac{m(1-\rho)^2 + 2\rho - (1-\rho)\sqrt{4m\rho + m^2(1-\rho)^2}}{-m\rho(1-\rho) + 2\rho + \rho\sqrt{4m\rho + m^2(1-\rho)^2}};$$

$$L = \left[\frac{m(1-\rho)^2 + 2\rho - (1-\rho)\sqrt{4m\rho + 4(m+1) + m^2(1-\rho)^2}}{-m\rho(1-\rho) + 2\rho + \rho\sqrt{4m\rho + 4(m+1) + m^2(1-\rho)^2}}\right]^+.$$

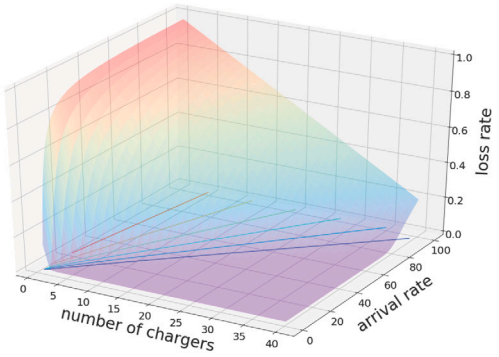

(a) Loss rate $f(\lambda, \mu, m)$ as function of m, λ, and μ.

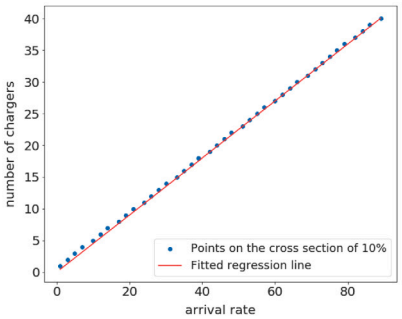

(b) $\alpha = 10\%$.

Fig. 2. Loss rate $f(\lambda, \mu, m)$ and the cross section with fixed loss rate.

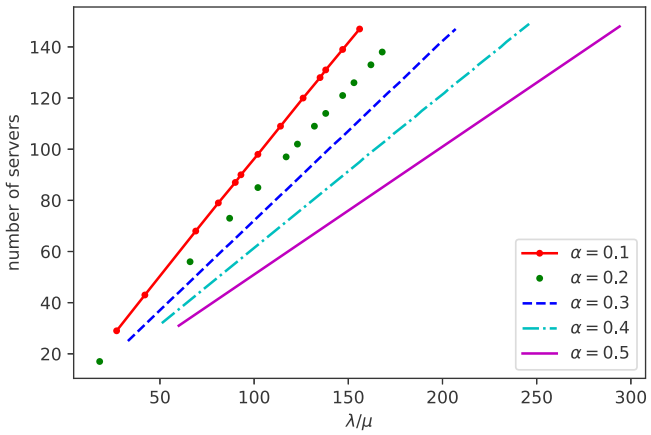

Fig. 3. Linear relationship between ratio λ/μ and the number of servers in an $M/G/m/m$ queue.

Thus, when m becomes large,

$$\lim_{m\longrightarrow\infty} U = \frac{(1-\rho)^2 - (1-\rho)\sqrt{(1-\rho)^2}}{-\rho(1-\rho) + \rho\sqrt{(1-\rho)^2}} = \begin{cases} \frac{\rho-1}{\rho}, \text{ if } \rho > 1; \\ 0, \text{ if } 0 < \rho \leq 1. \end{cases}$$

$$\lim_{m\longrightarrow\infty} L = \frac{(1-\rho)^2 - (1-\rho)\sqrt{(1-\rho)^2}}{-\rho(1-\rho) + \rho\sqrt{(1-\rho)^2}} = \begin{cases} \frac{\rho-1}{\rho}, \text{ if } \rho > 1; \\ 0, \text{ if } 0 < \rho \leq 1. \end{cases}$$

Therefore, $\lim_{m\longrightarrow\infty} f(\lambda, \mu, m) = (\rho - 1)/\rho = \alpha$, we have

$$\rho = \frac{\lambda}{m\mu} \longrightarrow \frac{1}{1-\alpha}, \quad \text{as} \quad m \longrightarrow \infty.$$

Proposition 3.1 suggests that in a time-independent queue with Poisson arrivals and generally-distributed service times of a certain service rate, the number of servers should change proportionally with the arrival rate to maintain the service level requirement α. Please note that the size of the queue can be as small as ten servers to be in compliance with the proposition, despite that the approximation of λ/m converges to the exact ratio of μ and $1-\alpha$ as the number of servers increase in the queue. Now we justify Proposition 3.1 in the following illustrative example.

Example. Consider a charging system following the $M/G/m/m$ queue with λ being the system arrival rate and μ being the service rate of each charger. First, we fix μ and enumerate the loss rate $f(\lambda, \mu, m)$, which is a function of λ and m of varied values as shown in Fig. 2(a). We then plot the cross section with $f(\lambda, \mu, m) = 90\%$ and $\epsilon = 0.001$ as shown in Fig. 2(b), where $R^2 = 0.9735$ in the linear regression demonstrates a sufficiently good fitness.

Keeping μ the same, we further plot the scatter chart of m and λ/μ for different loss rate $f(\lambda, \mu, m)$ in Fig. 3. Thus, we show the linear relationship between the ratio λ/μ and the number of servers m in an $M/G/m/m$ queue. For reasonably large numbers of servers and arrival rates, the slope of the line is equal to $1-\alpha$, as shown in (3).

Therefore, we can re-write the constraint (2b) as

$$\sum_{j\in J}\omega_j X_{ij} = \beta m_i, \quad \forall i \in I,$$

where $\beta := \mu\frac{1}{1-\alpha}$ is the coefficient determined by a specific loss rate α in Proposition 3.1. Thus, model (2) can be approximated by

$$\begin{aligned}
\min \quad & \sum_{i\in I} c m_i + \sum_{i\in I} s_i Y_i + \sum_{j\in J}\omega_j \sum_{i\in I} d_{ij} X_{ij} \\
\text{s.t.} \quad & \sum_{j\in J}\omega_j X_{ij} = \beta m_i, && \forall i \in I, \\
& \sum_{i\in I} X_{ij} \geq 1, && \forall j \in J, \\
& X_{ij} \leq Y_i, && \forall i \in I, j \in J, \\
& X_{ij}, Y_i \in \{0,1\}, m_i \in \mathbb{Z}_+, && \forall i \in I, j \in J,
\end{aligned} \tag{4}$$

3.3. Robust model and equivalent reformulation

Section 3.2 implies that model (2) can be approximated by model (4) with satisfactory fitness. Therefore, we next consider demand uncertainty in model (4), formulate the corresponding robust counterpart model, and derive the equivalent reformulation.

Consider the robust model with demand uncertainty, which is represented as $\tilde{\omega}_j$ and the corresponding vector is denoted by $\tilde{\boldsymbol{\omega}}$. Suppose the uncertain demand $\tilde{\boldsymbol{\omega}}$ lies in the following uncertainty set,

$$\Omega := \left\{ \tilde{\boldsymbol{\omega}} \middle| \begin{array}{ll} \tilde{\omega}_j = \bar{\omega}_j + \hat{\omega}_j z_j, & \forall j \in J, \\ 0 \leq |z_j| \leq 1, & \forall j \in J, \\ \sum_{j\in J} |z_j| \leq \Gamma & \end{array} \right\}$$

where $\bar{\omega}_j$ and $[\bar{\omega}_j - \hat{\omega}_j, \bar{\omega}_j + \hat{\omega}_j]$ represent the nominal value and the support of $\tilde{\omega}_j$, respectively. And Γ indicates the level of uncertainty for the charging demand. A large Γ value allows more deviation in the charging demand ω, compared with a small Γ. We study the impacts of Γ on the resulting robust optimums and values of objective function in sensitivity analysis (Section 4.4). Then the robust counterpart of model (4) is given by

$$\min \quad \sum_{i\in I} c_i m_i + \sum_{i\in I} s_i Y_i + \max_{\tilde{\boldsymbol{\omega}}\in\Omega} \sum_{j\in J} \tilde{\omega}_j \sum_{i\in I} d_{ij} X_{ij} \tag{5a}$$

$$\text{s.t.} \quad \max_{\tilde{\boldsymbol{\omega}}\in\Omega} \sum_{j\in J} \tilde{\omega}_j X_{ij} = \beta m_i, \qquad \forall i \in I, \tag{5b}$$

$$\sum_{i\in I} X_{ij} \geq 1, \qquad \forall j \in J, \tag{5c}$$

$$X_{ij} \leq Y_i, \qquad \forall i \in I, j \in J, \tag{5d}$$

$$X_{ij}, Y_i \in \{0,1\}, m_i \in \mathbb{Z}_+, \qquad \forall i \in I, j \in J, \tag{5e}$$

where the objective minimizes the cost of location and charger deployment and the worst-case travel time cost. The first and second constraints guarantee the feasibility for the worst-case scenario. In this model, the location, the charger deployment, and the demand allocation decisions are all made prior to any realization of uncertain data.

We next have the following theorem which shows that model (5) can be equivalently reformulated as a mixed integer linear program.

Theorem 3.1. *Model (5) can equivalently reformulated as*

$$\begin{aligned}
\min \quad & \sum_{i\in I} c_i m_i + \sum_{i\in I} s_i Y_i + Z \\
\text{s.t.} \quad & Z \geq \sum_{j\in J} \bar{\omega}_j \sum_{i\in I} d_{ij} X_{ij} + \upsilon\Gamma + \sum_{j\in J} u_j, \\
& \upsilon + u_j \geq \hat{\omega}_j \sum_{i\in I} d_{ij} X_{ij}, && \forall j \in J, \\
& \beta m_i \geq \sum_{j\in J} \bar{\omega}_j X_{ij} + p_i\Gamma + \sum_{j\in J} q_{ij}, && \forall i \in I, \\
& p_i + q_{ij} \geq \hat{\omega}_j X_{ij}, && \forall i \in I, j \in J, \\
& \sum_{i\in I} X_{ij} \geq 1, && \forall j \in J, \\
& X_{ij} \leq Y_i, && \forall i \in I, j \in J, \\
& X_{ij}, Y_i \in \{0,1\}, m_i \in \mathbb{Z}_+, && \forall i \in I, j \in J, \\
& Z, u_j, \upsilon, p_i, q_{ij} \geq 0, && \forall i \in I, j \in J.
\end{aligned} \tag{6}$$

Proof. First, the objective (5a) can be written as

$$\min \quad \sum_{i\in I} c_i m_i + \sum_{i\in I} s_i Y_i + Z$$

where

$$Z \geq \max_{\tilde{\omega}\in\Omega} \sum_{j\in J} \tilde{\omega}_j \sum_{i\in I} d_{ij} X_{ij} \tag{7}$$

Substituting the definition of uncertainty set Ω, constraint (7) can be written as

$$\begin{aligned} Z &\geq \max_{z_j\ \forall j\in J} \left\{ \sum_{j\in J} (\bar{\omega}_j + \hat{\omega}_j z_j) \sum_{i\in I} d_{ij} X_{ij} \middle| \begin{array}{l} \sum_{j\in J} |z_j| \leq \Gamma, \\ 0 \leq |z_j| \leq 1, \quad \forall j \in J, \end{array} \right\} \\ &= \sum_{j\in J} \bar{\omega}_j \sum_{i\in I} d_{ij} X_{ij} + \max_{z_j,\forall j\in J} \left\{ \sum_{j\in J} \hat{\omega}_j z_j \sum_{i\in I} d_{ij} X_{ij} \middle| \begin{array}{l} \sum_{j\in J} |z_j| \leq \Gamma, \\ 0 \leq |z_j| \leq 1, \quad \forall j \in J, \end{array} \right\} \end{aligned}$$

For the maximization subproblem as in the last term, we have

$$\begin{aligned} &\max_{z_j,\forall j\in J} \left\{ \sum_{j\in J} \hat{\omega}_j z_j \sum_{i\in I} d_{ij} X_{ij} \middle| \begin{array}{l} \sum_{j\in J} |z_j| \leq \Gamma, \\ 0 \leq |z_j| \leq 1, \quad \forall j \in J, \end{array} \right\} \\ &= \max_{z_j^+, z_j^-, \forall j\in J} \left\{ \sum_{j\in J} \hat{\omega}_j (z_j^+ - z_j^-) \sum_{i\in I} d_{ij} X_{ij} \middle| \begin{array}{ll} \sum_{j\in J} (z_j^+ + z_j^-) \leq \Gamma, & \\ z_j^+ + z_j^- \leq 1, & \forall j \in J, \\ z_j^+, z_j^- \geq 0, & \forall j \in J \end{array} \right\} \\ &= \min_{u_j, v, \forall j\in J} \left\{ v\Gamma + \sum_{j\in J} u_j \middle| \begin{array}{ll} v + u_j \geq \hat{\omega}_j \sum_{i\in I} d_{ij} X_{ij} & \forall j \in J, \\ v + u_j \geq -\hat{\omega}_j \sum_{i\in I} d_{ij} X_{ij} & \forall j \in J, \\ v, u_j \geq 0, & \forall j \in J \end{array} \right\} \\ &= \min_{u_j, v, \forall j\in J} \left\{ v\Gamma + \sum_{j\in J} u_j \middle| \begin{array}{ll} v + u_j \geq \hat{\omega}_j \sum_{i\in I} d_{ij} X_{ij}, & \forall j \in J, \\ v, u_j \geq 0, & \forall j \in J \end{array} \right\} \end{aligned}$$

where v and u_j denote the dual variables of the corresponding constraints, respectively. Thus, constraint (7) can be equivalently written as

$$\begin{aligned} & Z \geq \textstyle\sum_{j\in J} \bar{\omega}_j \sum_{i\in I} d_{ij} X_{ij} + v\Gamma + \sum_{j\in J} u_j, \\ & v + u_j \geq \hat{\omega}_j \sum_{i\in I} d_{ij} X_{ij}, && \forall j \in J, \\ & v, u_j \geq 0, && \forall j \in J. \end{aligned}$$

Similarly, constraint (5b) can be equivalently written as, for each $i \in I$,

$$\begin{aligned} \beta m_i &\geq \max_{\tilde{\omega}\in\Omega} \sum_{j\in J} \tilde{\omega}_j X_{ij} \\ &= \max_{z_j,\forall j\in J} \left\{ \sum_{j\in J} (\bar{\omega}_j + \hat{\omega}_j z_j) X_{ij} \middle| \begin{array}{l} \sum_{j\in J} |z_j| \leq \Gamma, \\ 0 \leq |z_j| \leq 1, \quad \forall j \in J, \end{array} \right\} \\ &= \sum_{j\in J} \bar{\omega}_j X_{ij} + \max_{z_j,\forall j\in J} \left\{ \sum_{j\in J} \hat{\omega}_j z_j X_{ij} \middle| \begin{array}{l} \sum_{j\in J} |z_j| \leq \Gamma, \\ 0 \leq |z_j| \leq 1, \quad \forall j \in J, \end{array} \right\} \end{aligned}$$

For the maximization subproblem as in the last term, we have

$$\begin{aligned} &\max_{z_j,\forall j\in J} \left\{ \sum_{j\in J} \hat{\omega}_j z_j X_{ij} \middle| \begin{array}{l} \sum_{j\in J} |z_j| \leq \Gamma, \\ 0 \leq |z_j| \leq 1, \quad \forall j \in J, \end{array} \right\} \\ &= \max_{z_j^+, z_j^-, \forall j\in J} \left\{ \sum_{j\in J} \hat{\omega}_j (z_j^+ - z_j^-) X_{ij} \middle| \begin{array}{ll} \sum_{j\in J} (z_j^+ + z_j^-) \leq \Gamma, & \\ z_j^+ + z_j^- \leq 1, & \forall j \in J, \\ z_j^+, z_j^- \geq 0, & \forall j \in J, \end{array} \right\} \\ &= \min_{p_i, q_{ij} \forall j\in J} \left\{ p_i \Gamma + \sum_{j\in J} q_{ij} \middle| \begin{array}{ll} p_i + q_{ij} \geq \hat{\omega}_j X_{ij} & \forall j \in J, \\ p_i + q_{ij} \geq -\hat{\omega}_j X_{ij} & \forall j \in J, \\ p_i, q_{ij} \geq 0, & \forall j \in J \end{array} \right\} \\ &= \min_{p_i, q_{ij} \forall j\in J} \left\{ p_i \Gamma + \sum_{j\in J} q_{ij} \middle| \begin{array}{ll} p_i + q_{ij} \geq \hat{\omega}_j X_{ij}, & \forall j \in J \\ p_i, q_{ij} \geq 0, & \forall j \in J \end{array} \right\} \end{aligned}$$

where p_i and q_{ij} represent the dual variables for the corresponding constraints, respectively. Thus, constraint (5b) can be equivalently written as

$$\begin{aligned} &\beta m_i \geq \sum_{j\in J} \bar{\omega}_j X_{ij} + p_i \Gamma + \sum_{j\in J} q_{ij}, && \forall i \in I, \\ &p_i + q_{ij} \geq \hat{\omega}_j X_{ij}, && \forall i \in I, j \in J, \\ &p_i, q_{ij} \geq 0, && \forall i \in I, j \in J. \end{aligned}$$

To conclude, model (5) can be equivalently written as in (6), which completes the proof.

Note that model (6) is a mixed integer linear program, which is tractable by many commercial solvers like Gurobi and CPLEX. In the following section, we solve model (6) by Gurobi and propose a simulation approach to evaluate the performance of the robust model under a real data set.

3.4. Benchmark: A corresponding stochastic model

Let $\boldsymbol{P}$ be the joint distribution of $(\tilde{\omega}_j \ \forall j \in J)$, so we can derive the stochastic model corresponding to model (4) as

$$\begin{aligned} \min \quad & \sum_{i\in I} cm_i + \sum_{i\in I} s_i Y_i + \mathbb{E}_{\boldsymbol{P}} \left[\sum_{j\in J} \tilde{\omega}_j \sum_{i\in I} d_{ij} X_{ij} \right] \\ \text{s.t.} \quad & \sum_{j\in J} \tilde{\omega}_j X_{ij} = \beta m_i, && \boldsymbol{P}\text{-a.s. } \forall i \in I, \\ & \text{(5c)–(5e)}. \end{aligned} \tag{8}$$

where $\boldsymbol{P}$-a.s. in the first constraint implies that the constraint must be satisfied almost surely under the probability measure $\boldsymbol{P}$. We next approximate model (8) by the Sample Average Approximation (SAA). For each sample $s = 1, \ldots, S$, denote p^s as the probability of sample such that $\sum_{s=1}^{S} p^s = 1$, and $(\omega_j^s \ \forall j \in J)$ as the demand in this scenario. Then the SAA reformulation of model (4) is as follows:

$$\begin{aligned} \min \quad & \sum_{i\in I} cm_i + \sum_{i\in I} s_i Y_i + \sum_{s=1}^{S} p^s \sum_{j\in J} \omega_j^s \sum_{i\in I} d_{ij} X_{ij} \\ \text{s.t.} \quad & \sum_{j\in J} \omega_j^s X_{ij} = \beta m_i, && \forall i \in I, s = 1, \ldots, S, \\ & \text{(5c)–(5e)}. \end{aligned} \tag{9}$$

4. Case study

In this section, we perform a case study using traffic flow data and power network information in the district of Luhe (also known as Liuhe). First, we describe our real traffic data in Section 4.1, followed by parameter estimation for the optimization models in Section 4.2. After presenting optimal allocations of charging stations in Section 4.3, we perform sensitivity analysis of varying uncertainties and charging demands in Section 4.4. Finally, we compare the optimums of our robust optimization model with deterministic and stochastic optimization models in a simulation study (Section 4.5). The simulation study also relax the assumption of time-independent charging demand in the optimization models.

4.1. Data description

Luhe, as shown in Fig. 4, is one metropolitan county of Nanjing, the capital of Jiangsu Province in Southeast China. With a population of approximately one million inhabitants, it covers an area of 1481 square kilometers, boasting a population density of 639 people per square kilometer[4]—figures comparable to medium-sized U.S. cities such as Austin, TX, Nashville, TN, and Jacksonville, FL.[5] Serving as the northern gateway to Nanjing, the provincial capital, Luhe has historically been a local focal point for economy, transportation, culture, and tourism. Notably, it forms part of the Nanjing Jiangbei New Area, featuring several burgeoning industrial parks.[6] The historic town of Luhe, nestled within the meandering curve of the Chuhe River, is easily accessible by ferry and metro. The southeast Lingyan Mountain contributes to the cultural and mythical traditions of the region.[7] In its province, EVs have been experiencing a surge in popularity, constituting about one-quarter of new vehicle registrations in 2022. Impressively, the province boasts over 9.9 million EVs as of 2022, reflecting a remarkable 96.3% year-to-year increase.[8] The City of Nanjing host

[4] See https://en.wikipedia.org/wiki/Nanjing#Demographics https://postal-codes.cybo.com/china/luhe-district/ (retrieved on 2023-11-21).
[5] See https://en.wikipedia.org/wiki/List_of_United_States_cities_by_population (retrieved on 2023-11-21).
[6] See https://english.nanjing.gov.cn/investment/keypark/201602/t20160202_1946071.html (retrieved on 2023-11-21).
[7] See https://isocarp.org/app/uploads/2016/01/ISOCARP-AfE-n3.pdf (retrieved on 2023-11-22).
[8] See https://www.thenanjinger.com/news/nanjing-news/how-many-cars-are-in-nanjing-and-how-many-are-electric/ (retrieved on 2023-11-22).

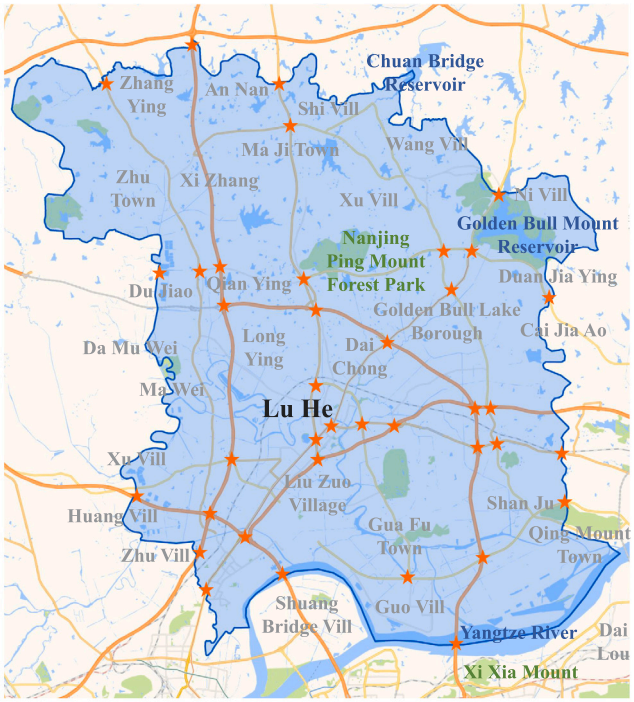

Fig. 4. The traffic network. The stars represent road segments of varying demand points.

several major Chinese EV manufacture sites, namely BYTON Auto Industry Park and ChangAn EV's factories.[9] While the city has been one of the leading cities in China receiving city-level government incentives since 2020,[10] Chinese government is planning to boost EV adoption in suburban areas like Luhe district.[11] The district also boasts robust electricity infrastructure exemplified by the renowned Yangba Power Station.[12]

In Luhe District, there are over 20 public charging stations, each equipped with at least four DCFCs.[13] The largest station boasts 20 DCFCs, all of which are in excellent working condition. These stations are managed by various chained EV charging companies, including Orange Unicorn, EV POWER, Star Charge, E-Charge by State Grid Corporation of China, among others. Based on interviews with industry professionals associated with these charging stations or their operating companies, it was revealed that one popular station, established in 2018, features eight DCFCs. This station consumed over 286,000 kilowatt-hours, achieving a power utilization rate of 90% (calculated as the ratio of actual charging capacity to rated power capacity). Another station, established in July 2023, houses four chargers and has serviced more than 8000 EVs. The utilization rate of its chargers surpasses 30%, signaling a significant demand and suggesting the need for additional chargers or charging stations.[14] Remarkably, with the exception of one station, all charging facilities are situated within 500 meters (approximately 0.3 miles) of the nearest road intersection. Furthermore, seven of these stations are directly positioned on land adjacent to road intersections.

The traffic flow data covers 46 segments of the first two levels of major roads, which include but are not limited to

1. Ningluo Expressway (G36),
2. Nanjing Ring Expressway (G2501),
3. Jiangbei Avenue Expressway,
4. Shanghai-Shaanxi Expressway (G40),
5. Changshen Expressway (G25),
6. Ninglian Expressway (G205),
7. Jinjiang Road, Changshen Bridge (S353),

[9] https://siteselection.com/issues/2019/jul/nanjing-china-a-one-stop-shop-for-new-energy-vehicles.cfm (retrieved on 2023-11-27).
[10] https://theicct.org/wp-content/uploads/2023/02/China-NEPC-city-policies_final.pdf (retrieved on 2023-11-27).
[11] https://senecaesg.com/insights/china-to-promote-ev-charging-infrastructure-targeting-rural-ev-market/ (retrieved on 2023-11-27).
[12] https://www.gem.wiki/Nanjing_Liuhe_District_Yangba_power_station (retrieved on 2023-11-27).
[13] https://www.google.com/maps/search/charging+station/@32.3213358,118.7233816,12z/data=!4m8!2m7!3m6!1scharging+station!2sLuhe+District,+Nanjing,+Jiangsu,+China!3s0x35b5fd7b45f8bd67:0xc176eaae1f573d8a!4m2!1d118.82155!2d32.3222199?authuser=0&entry=ttu (retrieved on 2023-11-27).
[14] https://evchargingsummit.com/blog/top-metrics-to-measure-the-performance-of-your-ev-charging-stations/ (retrieved on 2024-01-30).

8. Yanyang Road (S353),
9. G235 National Highway,
10. Eastern Main Line (S4210),
11. Liuhe Bridge (G328),
12. Ninghai Line,
13. Qinglu Line (S356),
14. Emei Road (S247).

And many more segments from other major roads are also included in the dataset. The studied area contains 39 road intersections in total identified by stars in Fig. 4. In this study, we designate road intersections as potential locations for EV charging stations. This is grounded in the observation that sites proximate to road intersections are commonly selected for DCFCs due to their inherent convenience. A pertinent example is the National Electric Vehicle Infrastructure (NEVI) Program, which mandates that EV charging infrastructure should be situated no more than one mile from interstates or highway intersections[15]—a regulation that aligns with similar guidelines established and implemented in the United States.[16] To specify, we designate road intersections as candidate spots for public EV charging stations, encompassing locations within a radius of 500 meters or 0.3 miles from the road intersections. This decision is informed by the observation that nearly all existing EV charging stations in the study area are situated within this proximity to their nearest road intersections. Please note that one limitation associated with placing charging stations near road intersections is the potential disruption to traffic flow caused by frequent car stops for charging. This has the potential to induce traffic jams and bottlenecks on highways. To address this concern, additional precautions should be exercised when siting charging stations near road intersections. This includes optimizing traffic signal timing, avoiding busy intersections with excess capacity, and strategically clustering charging stations at nearby intersections.[17] Despite that they are beyond the scope of this study, these measures are crucial to ensuring the seamless integration of EV charging infrastructure while mitigating any adverse impact on the efficiency of traffic flow. We also acknowledge that alternative locations suitable for EV charging stations encompass areas near transmission lines and substations,[18] existing parking lots, as well as traditional fuel or gas stations.[19] Our models and methods in Section 3 are adaptable and can be easily customized to consider diverse sets of candidate sites.

We use the Baidu map coordinate-picking system[20] to determine the latitudes and longitudes of these road segments and intersection, followed by collecting the real-time two-way traffic flow data on these road segments at the Baidu map open platform.[21] In particular, we develop a webpage on localhost with JavaScript codes, which allows us to request traffic data every 15 min from December 2018 to March 2020. The dynamics of traffic flows exhibit temporal variability. Typically, we commonly observe sluggish traffic during morning and afternoon peak periods on workdays, as well as in the periods preceding and following extended holidays. While our robust optimization approach (Section 3) adeptly addresses the variation range of the derived charging demand, it fails to fully encapsulate the real-time dynamics of traffic flows. Consequently, in Section 4.5, we employ a simulation approach to model the time-dependent charging demand. This approach intricately aligns with the temporal dynamics of traffic flow, providing a nuanced and temporally sensitive representation of the charging demand scenario.

4.2. Parameter estimation

To this end, we calibrate parameters in this case study based on real data. Table 2 provides a summary of the parameters along with their corresponding values or the sources from which these values are derived.

We refer the fixed cost s_i of setting up station i to the cost of building power lines to location i, which is proportional to the distance of location i to the nearest power substation with the unit cost being 20 Chinese Yuan (CNY) per meter. The unit cost c of setting up a charger in stations is set to 130,000 CNY.[22] For each charger following the general process to serve a customer, the service rate μ is set to 2, where the charging time is half an hour on average.[23] For the time cost d_{ij} of traveling from demand node j to station i to charge a vehicle, it is proportional to the distance from i to j, where the unit cost per km is calculated according to the average speed on expressways and the minimum hourly wage in Nanjing.[24]

Regarding the charging demand, we directly estimate expected value and variability of DC charging demand at point j based on traffic flow in the network. Let $\bar{v}$ be the average speed at a certain time on a specific road segment. $\bar{v}$ are rarely zero within 15-minute intervals in our data, despite of the fact the traffic may stop moving for a short period of time in practice. Thus, the expected number of vehicles $\bar{k}$ passing this segment in a unit time T can be estimated by

$$\bar{k} = \frac{T}{\bar{v}}.$$

[15] See https://blinkcharging.com/understanding-nevi-funding-for-ev-charging-infrastructure-along-americas-highways/ (retrieved on 2023-11-22).

[16] See https://www.route-fifty.com/infrastructure/2023/03/race-build-out-ev-charging-stations-some-cities-and-states-have-leg/383559/ (retrieved on 2023-11-21).

[17] See https://energy5.com/examining-the-effects-of-ev-charging-stations-on-traffic-signal-optimization (retrieved on 2023-11-22).

[18] See https://calstart.org/electric-highways-study/ (retrieved on 2023-11-27).

[19] See https://www.cnbc.com/2023/08/19/how-gas-station-economics-will-change-in-the-ev-charging-future.html (retrieved on 2023-11-21).

[20] See http://api.map.baidu.com/lbsapi/getpoint/index.html (retrieved on 2021-12-30).

[21] See http://lbsyun.baidu.com (retrieved on 2022-01-15).

[22] See https://www.gldjc.com/ for a website to inquiry the construction cost and the material price.(retrieved on 2021-12-30)

[23] See https://www.tesla.com for the average charging time.(retrieved on 2021-12-30)

[24] See http://jshrss.jiangsu.gov.cn/art/2021/7/28/art_77279_9953183.html for the standard of the minimum hourly wage in Nanjing.(retrieved on 2021-12-30)

Table 2
Notations for parameter estimation.

Parameter	Description	(Source of) Value
c	Unit cost of setting up a charger in stations	130,000 CNY
μ	Average service rate of a charger	2 vehicles per hour
α	Service level requirement	90%
T	A time period	15 min
p^s	Probability of a sample path	0.01
t	Spot time	Time-dependent
s_i	Fixed cost of setting up a charging station	Site-dependent
d_{ij}	Time cost of traveling	Footnote (20)
L	Length of a road segment	Footnote (20)
n	Number of lanes each way on the segment	Footnote (20)
$\bar{v}$	Average speed on a road segment	Footnote (21)
$\bar{k}$	Expected number of vehicles passing the segment	Footnote (21)
v_s	Spot speed on a road segment	Footnote (21)
v_j	Minimal speed on the road segment	Footnote (21)
v_c	Maximal speed on the road segment	Footnote (21)
k_j	Number of vehicles associated with v_j	Footnote (21)
k_c	Number of vehicles associated with v_c	Footnote (21)
k	Estimated number of vehicles	Footnote (21)
$\hat{\omega}_{j_t}$	Number of vehicles needing charging on road segment j at time t	Footnote (21)
ϕ	Charging rate, i.e., the proportion of vehicles needing on-route charging	1% (0.5%–10% in Section 4.4)
Γ	Uncertainty level	1 (1–14 in Section 4.4)

According to Notley et al. (2009), Jiming et al. (2017), and Funke et al. (2019), the number of vehicles on the road segment affects the spot speed v_s, together with minimal and maximal speeds—denoted by v_j and v_c, respectively—on a road segment, that is,

$$v_s = v_c - \frac{(v_c - v_j)\ln(k/k_c)}{\ln(k_j/k_c)},$$

where k_j and k_c are the number of vehicles associated with the minimal and maximal speeds. On the other hand, spot speed v_s can reversely affect the number of vehicles k, i.e.,

$$k = k_c \exp\left\{\frac{v - v_c}{v_j - v_c}\ln\frac{k_j}{k_c}\right\} \tag{10}$$

Suppose the length of the road segment is L, and there are n lanes each way on the road segment. At certain time point t, we can derive the number of vehicles k on one unit of road segment per unit of time based on (10). Therefore, the total charging demand at time t on that road segment across the time horizon of study T is estimated as

$$\hat{\omega}_{j_t} = \phi k L n T. \tag{11}$$

We take the mean and variance of all $\hat{\omega}_{j_t}$ over time as the expected value and the variability of charging demand in the robust optimization model. The charging rate ϕ refers to the percentage of vehicles requiring on-route charging service among all vehicles on the roads. Given historical traffic flow in this area, we project that $\phi = 1\%$ of these vehicles would be EVs that require on-route charging service in the near future. This estimation is due to several rationales. First, the private EV adoption in China has experienced remarkable growth. Although EVs accounted for 4.9% of all passenger vehicles in China, EV sales in China were more than double that of the US and Canada in 2022.[25] Secondly, the state of EV adoption in specific regions is also noteworthy. In 2017, California witnessed an EV adoption rate of approximately 5% according to Bellan (2018). Moreover, by the end of 2018, EV sales constituted over 10% of all passenger vehicles in Canada (Schmidt, 2019). Finally, we assume almost all EVs traveling in this inner-city urban transportation network rely only on DCFCs. This is due to the fact that almost all residences in the area are multi-story apartment buildings, making it impossible for EV users to charge at home. Given escalating EV adoption rates, we explore the optimal sizing and siting of charging stations under different charging rates in sensitivity analysis (Section 4.4).

4.3. Optimums

In this section, we present the solution of a robust model based on the case study. For comparison, we also find optimums to the two benchmarks corresponding to model (4)—the deterministic model and the stochastic model (8). The deterministic model is obtained by replacing each charging demand ω_j in (4) with the corresponding expectation. To solve model (9), we generate 100 scenarios with appropriately generated probability $p^s = 0.01$. For each scenario, the random demand ω_j^s are generated by a normal

[25] See https://en.wikipedia.org/wiki/Electric_car_use_by_country (retrieved on 2023-11-21).

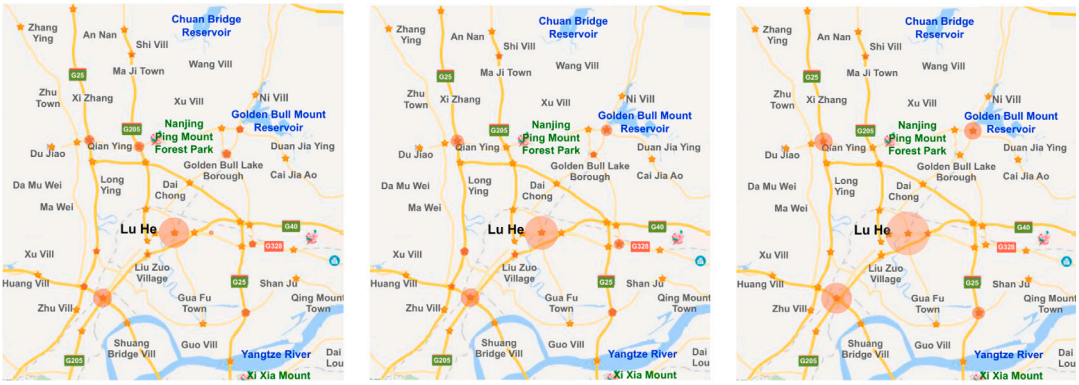

(a) Deterministic. (b) Stochastic. (c) Robust ($\Gamma = 1$).

Fig. 5. The optimum to the deterministic, stochastic, and robust optimization problem. The size of the red dots represent the number of chargers in the charging station, while the stars are the candidate stations without chargers in the optimum. (For interpretation of the references to color in this figure legend, the reader is referred to the web version of this article.)

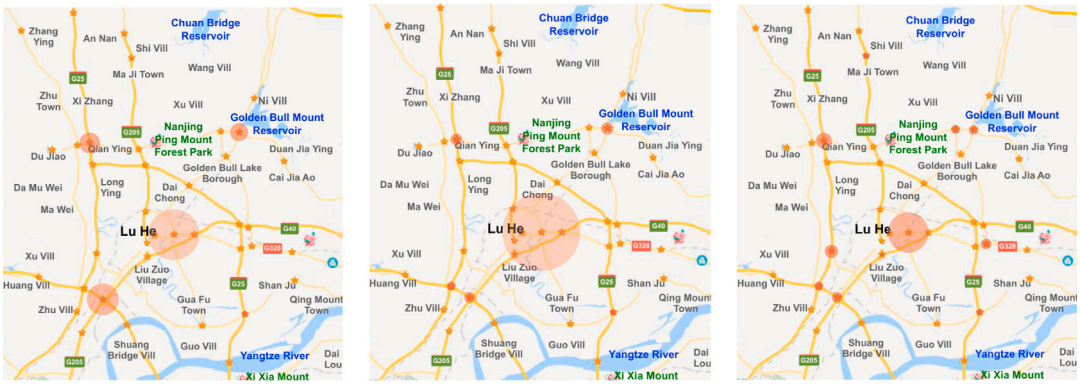

(a) $\Gamma = 1$. (b) $\Gamma = 7$. (c) $\Gamma = 14$.

Fig. 6. The optimum to the robust optimization problem under varying uncertainties. The size of the red dots represent the number of chargers in the charging station, while the stars are the candidate stations without chargers in the optimum. (For interpretation of the references to color in this figure legend, the reader is referred to the web version of this article.)

distribution of the same mean and standard deviation as the historical traffic flow data. Then model (9) is solved to obtain the stochastic optimums.

We solve the proposed robust optimization model (6) and two benchmark models by Gurobi 9.0.2 in `Python` 3.8.2. The results by three models are presented in Fig. 5, where we set $\Gamma = 1$ for the robust model. Compared with the deterministic and the stochastic models, the robust model leads to more allocated chargers in more scattered stations. This is because the robust model is required to be insensitive to uncertain charging demand, which seeks for more chargers to be allocated at more candidate stations in robust optimum than the those of deterministic and stochastic models.

4.4. Sensitivity analysis

We perform sensitivity analysis on the robust model with respect to uncertainties, i.e., the values of Γ. In Fig. 6, we present the solution to model (6) with the open charging stations represented by red dots when $\Gamma = 4, 7, 14$, and the size of dots corresponds to the number of chargers in the selected stations. Charging piles become more widely distributed when the value of Γ increases. Specifically, when $\Gamma \leq 7$, six charging stations will be established; when $7 \leq \Gamma \leq 14$, there would be 8 charging stations needed; and when $\Gamma \geq 14$, we would require 14 charging stations. Fig. 7 illustrates the change of total costs with respect to Γ. Uncertainty of demand can raise the total cost, because the total cost grows as the value of Γ increases. Moreover, in the three ranges ($1 \leq \Gamma \leq 6$, $7 \leq \Gamma \leq 14$ and $\Gamma \geq 14$), the total cost and Γ show nearly linear relationship. After reaching the critical value $\Gamma = 14$, the number of charging piles no longer increases, although the total cost slightly increases. This shows that when the uncertainty reaches a certain level, the robust optimization has reached the worst-case scenario and will not become worse. The growing cost is due to the travel time cost of EVs to charging stations only, and yet the infrastructure costs on power grid and chargers remain unchanged.

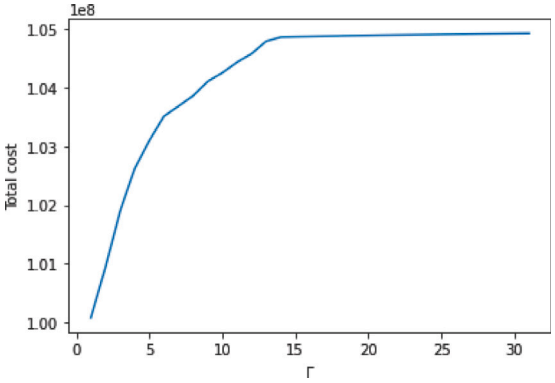

Fig. 7. Total costs with respect to different Γ values.

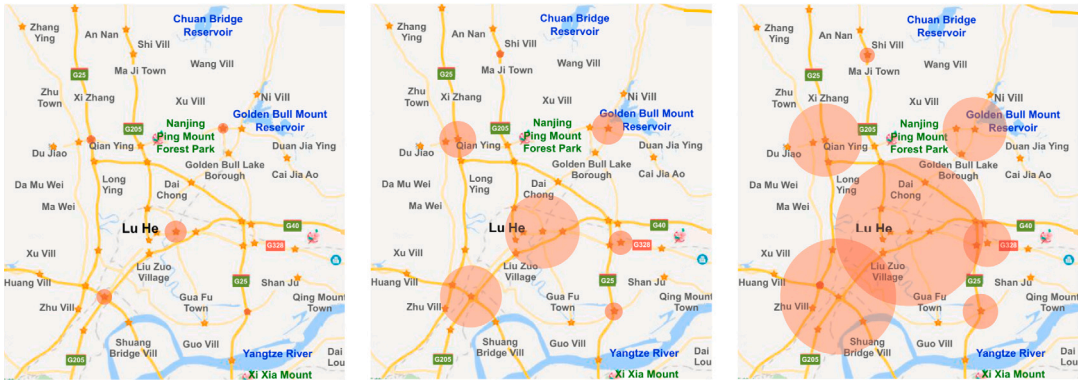

(a) $\phi = 0.5\%$. (b) $\phi = 2\%$ (c) $\phi = 4\%$

Fig. 8. The optimum to the robust optimization problem under varying charging rate, i.e., the proportion of traffic flow requiring on-route charging. The size of the red dots represent the number of chargers in the charging station, while the stars are the candidate stations without chargers in the optimum. (For interpretation of the references to color in this figure legend, the reader is referred to the web version of this article.)

Furthermore, we examine the optimal solution of the robust optimization problem under varying charging demands. With the proliferation of EV adoption, we note that the optimal sizes of charging stations exhibit an increase, while the optimal siting of charging stations remains relatively constant (Fig. 8). Additionally, our observations reveal a linear relationship between the penetration rates of EVs and the total optimal costs (Fig. 9).

4.5. Simulation

In this section, we first briefly introduce our simulation model and discuss our model validation, followed by two scenarios to verify effectiveness and efficiency of the deterministic, stochastic, and robust optimums mentioned beforehand. In this simulation study, we consider charging stations with time-dependent charging demand arrivals. That is, we relax the assumption of time-independent queues in the optimization models, providing insights regarding stations' allocation and deployment decisions in a realistic traffic setting.

4.5.1. Modeling framework

To assess the efficacy of the optimal solution within a practical transportation network, we develop a simulation model utilizing ARENA software version 16.0 (Rockwell). Our simulation is designed as a discrete event model, and it takes into account the presence of uncertain traffic intensity, which represents the fluctuating number of vehicles per unit length over a given period of time. This simulation is based on the following assumptions:

- At each road intersection, vehicles choose a specific turning direction, namely, go straight, turn left or right, with probabilities based on historical data observed in the modeled metropolitan area.

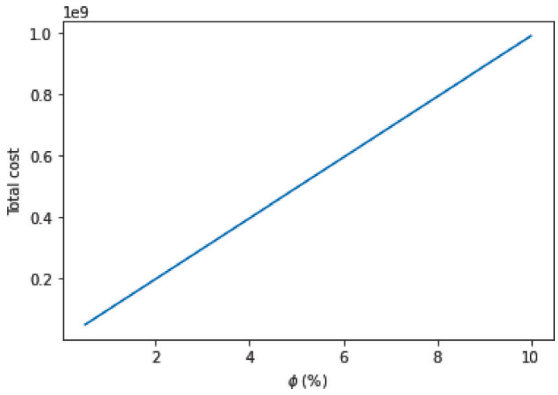

Fig. 9. Total costs with respect to different charging rates.

Table 3
Compare simulated and real traffic flows.

Road sections	Traffic flow (vehicles per day)		Percentage error
	Real data	Simulated	
Local	16,763	16,168	3.55%
Highway	12,344	12,733	3.15%

- No vehicles stop in the network unless for charging purposes at identified charging stations. In other words, there is no interruption of the traffic flow.
- Charging stations are independent queueing systems with chargers as servers.
- Vehicles' charging time follows an independent and identical triangular distribution, with a minimum time of 20 min, a maximum of 40 min and a mode—the most likely time required to charge a vehicle—of 30 min.
- The traffic is generated at source nodes located along the boundaries of the network under study.

Please note that the *source nodes* in the simulation models are different from the demand nodes in optimization models aforementioned. Now we explain how the "traffic amount" at source nodes (i.e., the number of vehicles per unit time from each source node) are generated in our discrete event simulation model. Each of the fourteen source nodes generates entities (i.e., EVs) in the network, based on traffic distributions estimated from historical data. Specifically, we first estimate vehicles' arrivals at each source node, and find time-dependent Poisson processes that fit their arrivals the best. Then we use ARENA's Schedule Data sheet module to incorporate these distributions in our simulation model. Vehicles are routed to different road segments following estimated probabilities. The movement of entities along each road segment is governed by specific speed distributions. These distributions are determined based on historical data and are fitted using MATLAB. These speed distributions are stored in an Arena 39×39 expression. Each time an entity enters a new road segment, it is assigned a speed following the speed distribution on that segment. We use ARENA's process modules to model charging activities at each charging station.

We perform model validation to make sure (1) that our simulation model integrates all specifications of the system under study, and (2) that it behaves as close as possible to the system under study. Specifically, we compare real traffic flows of the existing network to those generated by source nodes in the simulation model. Table 3 presents the traffic flows for two randomly selected road segments within the simulated network, representing one highway and one local road segment. The percentage of error displayed in Table 3 indicates minor discrepancies between the simulated and actual traffic flows. Consequently, the simulation model is deemed valid with a 95% level of confidence. Moreover, we use the animation of our model to attest that the simulated network is a reasonably close approximation of the existing network.

Considering that urban traffic in any modeled area runs in an infinite time horizon, we conduct analysis to determine the warm-up period for the model. Specifically, we first run 30 replications of the simulation model and analyze output statistics, including lengths of queues and number of entities in process of all replications, through the ARENA output analyzer. Our analysis shows that all replications reach a steady state after 5 days. Therefore, we identified a 5-day warm-up period followed by a 30-day simulation run length as the study period.

4.5.2. Scenarios and results

We use the following key performance indicators (KPIs) to evaluate the optimal solutions resulting from Section 3.

Service rate refers to the percentage of charging demand being fulfilled across all available charging stations. This represents the ratio of charged EVs to the total number of EVs that require charging at each station. This metric serves as a measure of the charging network's efficiency.

Table 4
Summarized simulation results for three optimization problems.

Optimization	Utilization (%)					Service rate (%)	
	<50	>75	>80	>85	Average	≥50	Average
Deterministic	77	13	13	13	21.75	31	29.27
Stochastic	82	8	5	5	15.72	26	24.60
Robust	15	77	77	72	85.76	72	70.57

Utilization (in %) is the fraction of time when a charger is charging EVs. This is a measure of effectiveness for the charging configuration.

In our simulation, we model the charging stations and their capacities resulting from deterministic, stochastic and robust optimization problems. Simulated EV users passing by a charging station have a fixed probability of charging their vehicles. If they choose to charge, they are served on a first-come-first-serve (FCFS) basis. In the case where all chargers in the chosen charging station are occupied, the EV will wait in the pooled queue, if the queue length at the charging station is constrained to be no greater than the number of available chargers. In simpler terms, we assume that EV drivers are willing to wait if, on average, there is no more than one vehicle in front of them for each charger. This assumption is reasonable considering clients' patience and the required time to charge an EV. When the number of EVs waiting for charging at the chosen station exceeds the number of available chargers, the EV user will opt to go to the second nearest charging station with available charging spots. To this end, with simulated traffic flow in the network that is very close to the reality, we are able to compare the efficiency and effectiveness of different configurations resulting from Section 3.

In Table 4, we present simulation results from three types of optimization. In the *Average* columns, we report the percentages of average utilization and average service rate across all proposed charging stations in the three optimums. Charging configuration resulting from robust optimization realizes an average utilization of over 85%, or four-folds for that of deterministic optimization and 5.5 times better than the stochastic method. The service rate for robust optimum is over 70%, more than double that of deterministic and almost three times that of the stochastic method.

In addition, we display the proportion of stations whose utilization is less than 50%, over 75%, more than 80% and beyond 85%. In the optimal charging network resulting from robust optimization, 72% of the charging stations have utilization over 85% and only 15% of the stations are utilized less than 50%. In contrast, 77% and 82% of charging stations are used less than 50% from the deterministic and stochastic optimizations, respectively. While most of the charging stations from deterministic and stochastic optimization are not well utilized, the sufficiently utilized stations (utilization rate over 80%) account for 13% in the deterministic method and only 5% for the stochastic method.

Moreover, we also show the proportion of charging stations having a service level of no less than 50%. In the robust optimal configuration, over 70% of the charging stations can fulfill at least half of their demand. Whereas fewer than one third of deterministic optimal stations and 26% of the stochastic ones can serve 50% of their charging demand. Therefore, we demonstrate that robust optimization outperforms deterministic and stochastic optimization to accommodate uncertain traffic flows and associated charging demand for public EV charging.

5. Conclusion

This forward-looking study aims to minimize the infrastructure costs of setting up public DCFC stations to meet emerging EV charging demand in any specific metropolitan area. Because of current extremely low adoption rates of EVs worldwide, it is impossible to gauge the exact charging demand or its distribution. Motivated by this challenge of unknown and uncertain charging demand, we develop a robust optimization problem with queue theory, after estimating the first and second moments of charging demand based on existing traffic flows in the transportation networks. To overcome the intractability of queueing constraints in the robust optimization, we figure out an approximate yet highly accurate linear relationship between the number of servers and arrival rates under any specific loss rate. Therefore, we can solve the deterministic dual of the original robust optimization, and hence find the optimum to the robust optimization problem.

Furthermore, we validate the optimum using a simulation approach, which takes into account more realistic factors, namely time-varying traffic flows and EV users' limited patience to wait for available chargers. The simulation approach finds that the realized utilization of chargers in the charging station layout determined by the robust optimization approach is very close to the targeted utilization rate.

Although our case study focuses on a specific metropolitan region in Southeast China, both our robust optimization and simulation approaches can be easily applied to other geographic areas. Nevertheless, our static models examine a single-epoch only. It is worthwhile for future research to investigate multiple-period decision making problems on public charging station allocation. Specifically, at each decision epoch, it is valuable to allocate charging stations with newly added chargers that satisfy constantly growing charging demand over time.

CRediT authorship contribution statement

Ting Wu: Writing – review & editing, Writing – original draft, Supervision, Resources, Methodology, Formal analysis, Data curation, Conceptualization. **Emily Fainman:** Writing – review & editing, Writing – original draft, Validation, Software, Project administration, Methodology, Formal analysis, Conceptualization. **Yasmina Maïzi:** Validation, Software, Methodology, Formal analysis. **Jia Shu:** Validation, Supervision, Project administration. **Yongzhen Li:** Writing – original draft, Methodology, Formal analysis.

Acknowledgments

Dr. Ting Wu's work was supported by the National Natural Science Foundation of China (No. 71971108), the Mathematics Tianyuan Fund of the National Natural Science Foundation of China (No. 12326321), and the Top Six Talents' Project of Jiangsu Province, China (No. XNYQC-001). Dr. Jia Shu's research was supported by the National Natural Science Foundation of China (No. 72091213 and 71831004) and the Fundamental Research Funds for the Central Universities, China. Dr. Yongzhen Li's research was supported by the National Natural Science Foundation of China (No. 72101056) and Southeast University Zhishan Young Scholar Program, China.

References

Arias, M.B., Bae, S., 2016. Electric vehicle charging demand forecasting model based on big data technologies. Appl. Energy 183, 327–339.
Arias, M.B., Kim, M., Bae, S., 2017. Prediction of electric vehicle charging-power demand in realistic urban traffic networks. Appl. Energy 195, 738–753.
Azadeh, S.S., Vester, J., Maknoon, M., 2022. Electrification of a bus system with fast charging stations: Impact of battery degradation on design decisions. Transp. Res. C 142, 103807.
Bae, S., Kwasinski, A., 2011. Spatial and temporal model of electric vehicle charging demand. IEEE Trans. Smart Grid 3 (1), 394–403.
Bandi, C., Bertsimas, D., Youssef, N., 2015. Robust queueing theory. Oper. Res. 63 (3), 676–700.
Basile, F., Chiacchio, P., Teta, D., 2012. A hybrid model for real time simulation of urban traffic. Control Eng. Pract. 20 (2), 123–137.
Bellan, R., 2018. The grim state of electric vehicle adoption in the U.S.. https://www.citylab.com/transportation/2018/10/where-americas-charge-towards-electric-vehicles-stands-today/572857/.
Berkelmans, G., Berkelmans, W., Piersma, N., Van Der Mei, R., Dugundji, E., 2018. Predicting electric vehicle charging demand using mixed generalized extreme value models with panel effects. Procedia Comput. Sci. 130, 549–556.
Bertsimas, D., Gamarnik, D., Rikun, A.A., 2011. Performance analysis of queueing networks via robust optimization. Oper. Res. 59 (2), 455–466.
Bertsimas, D., Sim, M., 2004. The price of robustness. Oper. Res. 52 (1), 35–53.
Bertsimas, D., Thiele, A., 2006. Robust and data-driven optimization: modern decision making under uncertainty. In: Models, Methods, and Applications for Innovative Decision Making. INFORMS, pp. 95–122.
Brandstätter, G., Leitner, M., Ljubić, I., 2020. Location of charging stations in electric car sharing systems. Transp. Sci. 54 (5), 1408–1438.
Breuer, L., 2008. Continuity of the M/G/c queue. Queueing Syst. 58 (4), 321–331.
Cai, H., Jia, X., Chiu, A.S., Hu, X., Xu, M., 2014. Siting public electric vehicle charging stations in Beijing using big-data informed travel patterns of the taxi fleet. Transp. Res. D 33, 39–46.
Cilio, L., Babacan, O., 2021. Allocation optimisation of rapid charging stations in large urban areas to support fully electric taxi fleets. Appl. Energy 295, 117072.
Dong, J., Liu, C., Lin, Z., 2014. Charging infrastructure planning for promoting battery electric vehicles: An activity-based approach using multiday travel data. Transp. Res. C 38, 44–55.
Funke, S.Á., Sprei, F., Gnann, T., Plötz, P., 2019. How much charging infrastructure do electric vehicles need? A review of the evidence and international comparison. Transp. Res. D 77, 224–242.
Ghamami, M., Zockaie, A., Nie, Y.M., 2016. A general corridor model for designing plug-in electric vehicle charging infrastructure to support intercity travel. Transp. Res. C 68, 389–402.
Habib, S., Khan, M.M., Hashmi, K., Ali, M., Tang, H., 2017. A comparative study of electric vehicles concerning charging infrastructure and power levels. In: 2017 International Conference on Frontiers of Information Technology. FIT, Institute of Electrical and Electronics Engineers, Inc., Islamabad, Pakistan, pp. 327–332.
Hall, D., Lutsey, N., 2017. Emerging Best Practices for Electric Vehicle Charging Infrastructure. Technical Report, The International Council on Clean Transportation (ICCT), Washington, DC, USA.
Harel, A., 1988. Sharp bounds and simple approximations for the Erlang delay and loss formulas. Manage. Sci. 34 (8), 959–972.
He, S.Y., Kuo, Y.-H., Wu, D., 2016. Incorporating institutional and spatial factors in the selection of the optimal locations of public electric vehicle charging facilities: A case study of Beijing, China. Transp. Res. C 67, 131–148.
Hokstad, P., 1978. Approximations for the M/G/m queue. Oper. Res. 26 (3), 510–523.
Hosseini, S., Sarder, M., 2019. Development of a Bayesian network model for optimal site selection of electric vehicle charging station. Int. J. Electr. Power Energy Syst. 105, 110–122.
Islam, M.M., Shareef, H., Mohamed, A., 2018. Optimal location and sizing of fast charging stations for electric vehicles by incorporating traffic and power networks. IET Intell. Transp. Syst. 12 (8), 947–957.
Jiming, H., Lingyu, K., Yaqi, S., Ying, L., Wenting, X., Hao, W., 2017. A review of demand forecast for charging facilities of electric vehicles. In: IOP Conference Series: Materials Science and Engineering. IOP Publishing, 012040.
Jung, J., Chow, J.Y.J., Jayakrishnan, R., Park, J.Y., 2014. Stochastic dynamic itinerary interception refueling location problem with queue delay for electric taxi charging stations. Transp. Res. C 40, 123–142. http://dx.doi.org/10.1016/j.trc.2014.01.008.
Kchaou-Boujelben, M., 2021. Charging station location problem: A comprehensive review on models and solution approaches. Transp. Res. C 132, 103376.
Khazaei, H., Misic, J.V., Misic, V.B., 2011. Modelling of cloud computing centers using M/G/m queues. In: International Conference on Distributed Computing Systems Workshops.
Khazaei, H., Misic, J., Misic, V.B., 2012. Performance analysis of cloud computing centers. IEEE Trans. Parallel Distrib. Syst. 23 (5), 936–943.
Kimura, T., 1983. Diffusion approximation for an M/G/m queue. Oper. Res. 31 (2), 304–321.
Kınay, Ö.B., Gzara, F., Alumur, S.A., 2021. Full cover charging station location problem with routing. Transp. Res. B 144, 1–22.
Li, M., Jia, Y., Shen, Z., He, F., et al., 2016. Strategic Charging Infrastructure Deployment for Electric Vehicles. Technical Report, California. Department of Transportation.

Li, N., Jiang, Y., Zhang, Z.-H., 2021. A two-stage ambiguous stochastic program for electric vehicle charging station location problem with valet charging service. Transp. Res. B 153, 149–171.
Li, J., Xie, C., Bao, Z., 2022. Optimal en-route charging station locations for electric vehicles: A new modeling perspective and a comparative evaluation of network-based and metanetwork-based approaches. Transp. Res. C 142, 103781.
Maïzi, Y., Zhu, E.C., Wu, T., Zhou, J., 2019. A reliable deployment strategy for public electric vehicle charging stations: A discrete event simulation model for power grid and traffic networks. In: 2019 Winter Simulation Conference. WSC, IEEE, pp. 1660–1671.
Mak, H.-Y., Rong, Y., Shen, Z.-J.M., 2013. Infrastructure planning for electric vehicles with battery swapping. Manage. Sci. 59 (7), 1557–1575.
Mallig, N., Heilig, M., Weiss, C., Chlond, B., Vortisch, P., 2016. Modelling the weekly electricity demand caused by electric cars. Future Gener. Comput. Syst. 64, 140–150. http://dx.doi.org/10.1016/j.future.2016.01.014.
Marmaras, C., Xydas, E., Cipcigan, L., 2017. Simulation of electric vehicle driver behaviour in road transport and electric power networks. Transp. Res. C 80, 239–256. http://dx.doi.org/10.1016/j.trc.2017.05.004.
Notley, S., Bourne, N., Taylor, N., 2009. Speed, Flow and Density of Motorway Traffic. TRL INSIGHT REPORT.
Pourgholamali, M., Homem de Almeida Correia, G., Tarighati Tabesh, M., Esmaeilzadeh Seilabi, S., Miralinaghi, M., Labi, S., 2023. Robust design of electric charging infrastructure locations under travel demand uncertainty and driving range heterogeneity. J. Infrastruct. Syst. 29 (2), 04023016.
Quddus, M.A., Shahvari, O., Marufuzzaman, M., Ekşioğlu, S.D., Castillo-Villar, K.K., 2021. Designing a reliable electric vehicle charging station expansion under uncertainty. Int. J. Prod. Econ. 236, 108132.
Schiffer, M., Walther, G., 2018. Strategic planning of electric logistics fleet networks: A robust location-routing approach. Omega 80, 31–42.
Schmidt, E., 2019. Electric vehicles sales update Q3 2018, Canada. https://www.fleetcarma.com/electric-vehicles-sales-update-q3-2018-canada/.
Setiawan, A.D., Zahari, T.N., Anderson, K., Moeis, A.O., Hidayatno, A., 2023. Examining the effectiveness of policies for developing battery swapping service industry. Energy Rep. 9, 4682–4700.
Shanmukhappa, T., Ho, I.W.H., Tse, C.K., 2018. Spatial analysis of bus transport networks using network theory. Physica A 502, 295–314. http://dx.doi.org/10.1016/j.physa.2018.02.111.
Shen, Z.-J.M., Feng, B., Mao, C., Ran, L., 2019. Optimization models for electric vehicle service operations: A literature review. Transp. Res. B 128, 462–477.
Shortle, J.F., Thompson, J.M., Gross, D., Harris, C.M., 2018. Fundamentals of Queueing Theory, fifth ed. John Wiley & Sons.
Sun, H., Yang, J., Yang, C., 2019. A robust optimization approach to multi-interval location-inventory and recharging planning for electric vehicles. Omega 86, 59–75.
Thomin, P., Gibaud, A., Koutcherawy, P., 2013. Deployment of a fully distributed system for improving urban traffic flows: A simulation-based performance analysis. Simul. Model. Pract. Theory 31, 22–38.
Tijms, H.C., Hoorn, M.H.V., Federgruen, A., 1981. Approximations for the steady-state probabilities in the M/G/c queue. Adv. Appl. Probab. 13 (1), 186–206.
Union of Concerned Scientists, 2018. Electric vehicle charging: Types, time, cost and savings. https://www.ucsusa.org/resources/electric-vehicle-charging-types-time-cost-and-savings.
Wang, H., Zhao, D., Meng, Q., Ong, G.P., Lee, D.-H., 2019. A four-step method for electric-vehicle charging facility deployment in a dense city: An empirical study in Singapore. Transp. Res. A 119, 224–237.
Whitt, W., You, W., 2018. Using robust queueing to expose the impact of dependence in single-server queues. Oper. Res. 66 (1), 184–199.
Wolbertus, R., Kroesen, M., van den Hoed, R., Chorus, C., 2018. Fully charged: An empirical study into the factors that influence connection times at EV-charging stations. Energy Policy 123, 1–7.
Xi, X., Sioshansi, R., Marano, V., 2013. Simulation–optimization model for location of a public electric vehicle charging infrastructure. Transp. Res. D 22, 60–69.
Xie, F., Liu, C., Li, S., Lin, Z., Huang, Y., 2018. Long-term strategic planning of inter-city fast charging infrastructure for battery electric vehicles. Transp. Res. E 109, 261–276.
Yang, W., 2018. A user-choice model for locating congested fast charging stations. Transp. Res. E 110, 189–213.
Yang, J., Dong, J., Hu, L., 2017. A data-driven optimization-based approach for siting and sizing of electric taxi charging stations. Transp. Res. C 77, 462–477.
Yao, D.D., 1985. Refining the diffusion approximation for the M/G/m queue. Oper. Res. 33 (6), 1266–1277.
Yi, Z., Liu, X.C., Wei, R., 2022. Electric vehicle demand estimation and charging station allocation using urban informatics. Transp. Res. D 106, 103264.
Yılmaz, H., Yagmahan, B., 2022. Range coverage location model: An optimization model for the charging station location problem in a transportation network to cover intercity travels. Int. J. Energy Res. 46 (2), 1538–1552.